Statement of originality of the MSc thesis

I declare that:

1. this is an original report, which is entirely my own work,
2. where I have made use of the ideas of other writers, I have acknowledged the source in all instances,
3. where I have used any diagram or visuals I have acknowledged the source in all instances,
4. this report has not and will not be submitted elsewhere for academic assessment in any other academic course.

Student data

Name: Richard Bakker
Registration number: 3279510

Surface uplift in world's youngest orogen, can crustal thickening explain the uplift in Timor?

R. R. Bakker.

MSc. Student, Geology, Earth Science, Utrecht University.

Abstract

The island of Timor, SE Asia is the result of Arc-continent collision of the Banda Arc with the Australian Continental margin. Shortening of the Australian plate strata leads to thickening of the crust. Assuming isostasy, this should cause uplift. We hypothesize that the uplift of Timor can be explained by the built-up of a fold-and-thrust belt. During this built up sedimentation of basins which structurally lie on top of this fold-and-thrust belt, was taking place. These syn-orogenic basins, known as the Viqueque formation, are passive recorders of the uplift history. We reconstruct the uplift history by building an age model for the Viqueque formation and using occurrences of depth markers (benthic foraminifera). Combining the age model with depth differences allows us to reconstruct the uplift history. Timor has experienced uplift in two phases: a phase with almost no significant uplift and generally very low uplift rates during the deposition of the lower part of the Viqueque formation, followed by a phase of rapid uplift, up to ~3 mm/yr. The fold-and-thrust belt has been thickened by an average thickening factor of 3.3. If we assume Airy-type isostasy, and that thickening starts around the first deposition of Viqueque strata, we find a theoretical uplift rate of around ~0.4 mm/yr. Homogeneous thickening of the fold-and-thrust belt alone might be enough to explain the low uplift rates in the lower part of the Viqueque formation. But it is not enough to explain the phase of rapid uplift. Another process is likely the cause for the observed uplift. Activation of the Wetar thrust might explain the uplift, but this is poorly constraint. Slab detachment is unlikely the cause because there is no evidence that the slab has broken off. Timor's position in the Banda-Arc Australia collision zone makes delamination the most likely process. But further research is needed to strengthen this hypothesis.

1. Introduction

Earth's topography has a very irregular distribution on its surface. Generally topographic differences exist in places where the lithosphere is deformed. Shortening results in crustal thickening forming high topography, and stretching leads to crustal thinning forming depressions.

However, topography may also result from large-scale flow in the mantle, with lithosphere overlying downwelling mantle getting depressed, and overlying upwelling mantle becoming elevated (dynamic topography e.g. Braun 2010). Unraveling tectonic and dynamic causes of topography proves to be problematic: many mountain ranges present a topography that cannot be straightforwardly explained by their crustal thickness (e.g. Atlas Mountains (Ayarza et al., 2005; Zeyen et al., 2005), Tien Shan (Burov et al., 1990)). If we can determine uplift rates on a developing mountain belt, where we know the contemporaneous crustal thickening, and compare these constraints with theoretical models, we can test the direct relationship between crustal thickening and uplift/topography. In other words, we can test whether crustal thickening alone is sufficient to explain the topography.

The island of Timor is a relatively small island and has a topography exceeding 3 km. It is one of Earth's youngest orogens, and resulted from collision between the underriding Australian

continent and the overriding oceanic Banda plate and overlying Arc (Harris, 2006). Timor exposes a fold-and-thrust belt of rocks derived from the Australian shelf, which were shortened by roughly 400 km (Tate et al., 2010). Deep marine basins from Latest Miocene to Pliocene age (Audley-Charles, 1967; Haig & McCartain, 2007) lie unconformable on top of the fold-thrust belt. This implies that initial folding has taken place before the sedimentation of these basins. The sediments are interpreted to be deposited during ongoing collision. Therefore these basins are also described as 'synorogenic basins' (Audley-Charles, 1967). Previous work has suggested that these basins recorded the uplift history of Timor (de Smet et al., 1990; Roosmawati & Harris, 2005; Haig & McCartain, 2007).

Because the uplift of Timor is very young, these erosion-prone basins have been preserved in various locations on the island, and their young age allows high-resolution dating of their stratigraphy. The tectonic setting on Timor is relatively straightforward. There are no present day tectonic structures present, which can cause topography other than the Australia-Banda collision. To summarize: Timor is young, has synorogenic basins and has a known shortening history. This makes Timor an excellent natural laboratory to study the relation between shortening and topography.

This study focuses on the uplift history of Timor during the formation of the highly deformed fold-and-thrust belt. We use the example of Timor to study the relation between crustal thickening and uplift, and propose that the uplift of Timor can be explained by isostatic effects due to the emplacement of the fold-and-thrust belt. To this end, we need to constrain the uplift history as it is recorded in the synorogenic sediments and create a model to find out what the theoretical uplift would be. Comparing the two results allows us to check whether our hypothesis is plausible.

The uplift history from the basins is derived using an age model, and depth estimates from benthic foraminiferal species. We build an age model based on biostratigraphy (first and last occurrences of planktonic foraminiferal species) and magnetostratigraphy (polarity reversals). Two locations are sampled for bio- and magnetostratigraphy in East Timor. The theoretical model is built based on isostatic equilibrium and homogeneous thickening of the fold-and-thrust belt. We therefore need to know when shortening (thickening of the fold-and-thrust belt) started and how much thickening there is at present day to construct a thickening factor history.

2. Geological Setting

2.1 Timor

The description of Timor's geology has been divided following political borders. Pioneering work in West (Dutch) Timor was carried out by Molengraaff (1912) and van Bemmelen (1949). East (Portuguese) Timor was first mapped and described by Audley-Charles (1968). During Indonesian occupation no field studies were allowed with a few exceptions for oil and gas explorations. Since East Timor's independence field studies were allowed again.

Timor is the result of active Arc-Continent collision (Audley-Charles, 2004). Intra-oceanic subduction changed to Arc-Continent collision when the Australian continental shelf entered the subduction zone (Harris et al., 1998 and references therein). In general Timor can be divided into two structural units: Asian- and Australian plate affinity. The Asian plate is the overriding, the Australian plate underriding. Both can be found in the tectonostratigraphy of the island: the underplated Australian shelf sediments have detached from the basement and now form a fold-

and-thrust belt (e.g. thin skinned tectonics; Charlton et al., 1991) and are the lowest tectonostratigraphic units on the island of Timor. On top of the fold-and-thrust belt lies another decollemant, which is formed by a tectonic mélange. This mélange is overthrusted by the metamorphic equivalents of the sediments which make up the fold-and-thrust belt (Aileu Fm.). The highest tectonostratigraphic unit is the Banda terrane (Harris, 2006) which has overthrusted the metamorphic Aileu Fm.

The Australian continental shelf sediments are also known as the Gondwana Sequence (Harris, 2006). This sequence consists of Permian to Jurassic strata. It has the Cribas formation at the base, a formation of shales and sandstones. Above lie the Triassic bedded limestone of the Aitutu formation. The youngest strata are Jurassic scaly clays of the Wailuli formation. The fold-and-thrustbelt is primarily built from Cribas and Aitutu formations. The Wailuli scaly clays are mechanically very weak and take up a lot of internal deformation (Tate et al., 2010). Locally this formation acts as the upper decollemant of the fold-and-thrust belt. Harris et al. (1998) have identified the scaly clays from the Wailuli formation as the matrix of the tectonic mélange (Bobonaro formation). In the Bobonaro formation, fragments of both tectonostratigraphically higher and lower units are found. Therefore Harris et al. argue the mélange is the result of exhumed material from the subduction channel.

The Aileu formation lies on top of the tectonic mélange. It consists of shales, slates, phyllites and quartzite in a South to North increasing trend of metamorphic grade (Tate et al., 2010). Metamorphic facies range from upper greenschist to amphibolite facies (Earle, 1981). Locally gabbroic intrusions can be found cross-cutting the metamorphic rocks. These have been dated at 8-5 Ma (Berry & McDougall, 1986). On top of the Aileu formation lie klippen of Banda Terrane (Harris, 2006), which is the only Asian affinity on Timor.

It is important to note that on top of the Wailuli fm. there used to be younger strata. These Cretaceous and younger strata are known as the Kolbano formation. However in East Timor, these are not found. In West Timor, these strata are found as another fold and thrust belt which lies on top of the mélange. In East Timor, in the same repetitions have been identified in seismic profiles in the Timor sea (Charlton et al., 1991). The stratigraphy which was on top of the Wailuli formation is thus now duplexed in a submarine fold and thrustbelt. On top of the Wailuli on East Timor, the Aileu formation and Banda Terrane are thrusted over.

Tate et al. (2010) have conducted detailed mapping of the fold-and-thrust belt and created balanced cross sections. (see figure 3). With these, they were able to find shortening rates for the Banda Arc-Australia collision. We can use the same numbers to find out by how much the fold-and-thrust belt has thickened. For the transect “Liquica-Ainaro”: the restored section was 512 km, the deformed and 156 km . This results in a thickening factor of 3.28. For the transect “Dili-Barique”: 597 km restored, 181 km deformed: thickening factor 3.30.

2.2 Viqueque Formation.

In the East of Timor, everything younger then Jurassic is missing, except for the Viqueque formation., which lies unconformable on the Bobonaro tectonic mélange (Audley-Charles, 1967). This formation can be found on various locations across the island, and consists of pelagic limestone, grading into marls at the base, followed by an irregular alternation of shale, silt, sand, gravel and conglomerates up to the top of the section. The conglomerates contain rounded pebbles of metamorphic phyllites and have been interpreted as turbidites and debris flows

(Audley-Charles, 1967; Haig & McCartain, 2007). The same studies have given the Viqueque Formation the rough age of Upper Miocene to Pliocene. Haig & McCartain (2007) have found the base of the formation to have an age between 5.6 and 5.2 Ma, and the top of the section has an age younger than 3.12 Ma. These results are based on biostratigraphy.

Both Audley-Charles (1967) and Haig & McCartain (2007) have indicated that sedimentation of these basins must have taken place during the orogenic process which build Timor. Both name the base of the Viqueque Formation a minimum age for the start of colliosion. Haig & McCartain (2007) use the presence of coastal foraminifera in turbidites as an indication for a emerging island. Audley-Charles (1967) interprets the differences in sedimentation rates (alternations of shale and sand) to periods of rapid erosion, due to periodic uplifts, due to the orogeny on Timor.

At present the Viqueque formation's strata lie tilted at shallow angles due to further uplift and mud diapirism of the Bobonaro Melange (Audley-Charles, 1986).

2.3 Sampling location

In order to study the above described processes, we have selected two sample sites. The two sections can be checked for internal consistency and provide clues on lateral differences. The two sites are 114.3 km apart at a strike of 85°, roughly the strike of the orogen. Both sites are outcrops along rivers: 1) Viqueque Type Section, from S08°51'54.6"; E126°21'48.7" (base) to S08°52'03.9"; E126°22'11.7" (top) and 2) Caiaco River Section, from S08°57'18.3"; E125°19'36.2 (base) to S08°58'12.7"; E125°18'55.2" (top), see figure 2B.

The Viqueque Type section can be found at the southern entrance of Viqueque, Central East Timor. We chose this location to compare our findings with earlier published results (Haig and McCartain, 2007). At this location approximately 250 m of continuous stratigraphy is logged. For both biostratigraphy and magnetostratigraphy 122 samples are taken. We achieve an average sampling density of 1 sample per 2 meters, which is necessary to pin point magnetic reversals and first/last occurrences of foraminifera species. At the base of the section (palegic marls) the sampling frequency was higher (2 samples per meter) to compensate for lower sedimentation rates.

The Caiaco River section site was chosen in the west of East Timor, near the town of Maliana. We chose this site because the thicker stratigraphy and to correlate our results with Duffy et al. (in preparation). We were able to log approximately 500 m of composite stratigraphy. Unfortunately the Viqueque Fm. was not continuous at this site. We have taken 120 samples for magnetostratigraphy, with an average sampling density of 1 per 2 meters (corrected for "not exposed" gaps). For biostratigraphy 78 samples were taken. As with the Viqueque Type section, we have increased the sampling density at the base of the section.

3. Materials and methods

3.1 Sampling and analytical techniques

For both sections, we have primarily used shale horizons as sample levels. Shales generally yield the highest foraminifera content. In addition, shales have been subjected little to no compaction. Thus the magnetic inclination is respectively slightly to not altered.

The samples for biostratigraphic interpretation consist of small rocks derived from the sample level. These samples were put in water with some hydrogen peroxide for a couple of days to fall

apart. The residue were washed using 600 and 125 µm sieves. The 125 µm fraction was dried and analyzed. We chose this fraction in order to compare our findings with van Marle (1989). Samples from the Viqueque Type section were used in order to compare with studies on the same section (e.g. Haig & McCartain, 2007). Occurrences of both planktonic and benthic species were logged. We the ratio between the planktonic and benthic spiecies occurrence within samples to constrain depth, in addition to depth markers (benthic species).

For paleomagnetic interpretations two cores per sample level were drilled using a gasoline powered, water cooled drill. All the biostratigraphic sample levels coincide with a paleomagnetic sample level. But for the Caiaco River section we took extra paleomagnetic samples to maintain a high enough sample resolution. For each sample we need to remove the overprint caused by the present day magnetic field to find the original magnetic direction (e.g. the magnetic field during deposition). This can be achieved by stepwise demagnetization. The overprint is generally due to magnetic carriers which can change their magnetic direction easily. These carriers are demagnetized at the lower demagnetization steps, leaving the original magnetic direction behind. Two methods of demagnetization were attempted: Thermal (th) and alternating electromagnetic field (af).

Thermal demagnetization was carried out using a magnetically shielded oven. Based on the results of the thermomagnetic runs (see figure 7 for an example), temperature increments range between 20-50 degrees, up to a maximum of 400 degrees, and a higher resolution (20 degrees increments) between 200 and 350 degrees. The samples were, after each temperature step, measured on a 2G enterprises horizontal DC SQUID cryogenic magnetometer. Between measurements the samples were kept in a magnetically shielded tube. AF-demagnetization was carried out in a magnetically shielded room (residual field <200 nT) by a robotized sample handler (Mullender et al., unpublished results), which also measures the samples after each demagnetization step using a 2G Enterprises SQUID magnetometer (noise level 1 x 10^{-12} Am^2).

4. Results

To constrain the uplift history we need to know ages and depths. We have built independent age models based on the different techniques. This interdisciplinary approach allows a higher certainty than using just one of the two methods. We will first show the results of the biostratigraphy, than the magnetostratigraphy and then compare the two. Biostratigraphy is only available for the Viqueque Type section. Samples from the Caiaco River section were not available before the writing of this thesis.

4.1 Biostratigraphy

Analysis of foraminifera allows us to get additional age constraints based on first and last evolutionary occurrences (resp. FO and LO). We used FO and LO ages for planktonic species from Wade et al. (2011) and the timescale of Lourens et al. (2004). Diagnostic planktonic species were: *Dentoglobigerina altispira* (pacific) (LO: 3.47Ma), *Globorotalia tumida* (pacific) (FO: 5.57 Ma), *Pulleniatina primalis* (FO: 6.60 Ma, LO 3.66 Ma), *Globorotalia crassaformis* (FO: 4.31 Ma), *Sphaeroidinella dehiscens* (FO: 5.53 Ma), *Globigerinoides conglobatus* (FO: 6.20 Ma) and *Sphaeroidinellopsis seminulina* (Pacific), (LO: 3.59 Ma). For an overview see figure 11.

Benthic species were used to determine paleobathymetry using the depth markers of van Hinsbergen et al. (2005). In the lower part, *Cibicides bradyi*, *Cibicides wuellerstorfi*, *Oridorsalis* and *Karreriella* are regularly present. Around 17m from the base, *Gyroidina* appears. This

indicates a depositional depth of >750m. More up in the stratigraphy, up from 40m, there is a regular presence of *Gyroidina*, *Uvigerina*, and of *Cibicides ungarianus.* This suggests a depth range of 350-750 m (upper-middle bathyal). Combined we find a gradual shift from lower to middle bathyal to middle to upper bathyal. Figure 12 shows an overview of the occurrences in the stratigraphy.

The ratio between the relative occurrence of planktonic and benthic foraminifera (e.g. van Marle, 1989; van Hinsbergen et al., 2005) was also determined. All samples had more than 95% planktonic foraminifera, indicating that during deposition the basin was at all time deeper than 1km (using equation (1) in van Hinsbergen et al., 2005).

4.2 Magnetostratigraphy

Alternating field demagnetization steps showed no clear consistent pattern when comparing samples. Thermomagnetic runs (figure 7) were conducted to see which thermal demagnetization steps were best to use. Figure 7 shows the typical irreversible decrease in between ~250 and ~350 °C. This indicates greigite as the main carrier of the magnetic signal. The irreversible decrease is caused by the alteration of greigite to sulphur, pyrite, marcasite and pyrrhotite (Skinner et al., 1964; Krs et al., 1992; Dekkers et al., 2000). Further oxidative alteration occurs around the 400 degrees. With this alteration new magnetic material is created of higher magnetic moment than what's left in the sample. With this process the directional properties of the original signal can no longer be accurately determined.

Results vary strongly between samples. In general, the intensity of the magnetic carriers was very low. A normal polarity component is removed at low temperature steps (100-200 °C). This is likely the present day field component. Determining the direction of this component without correction for tilt (no tc) resulted in an inclination which coincides with the present day field. For Timor, this is about -16° (up).

After removal of this component, the remaining intensity and direction is in most cases high enough to determine whether the original component is of a normal or reversed polarity. Figure 8 shows demagnetization diagrams (Zijderveld, 1967) of typical samples. Sample VT63 (see caption) shows a clear reversed polarity after the removal of the normal component. Sample VT80 (lowermost panels, see caption) show a clearly identifiable normal component. In some cases, the characteristic remnant magnetization (ChRM) direction could be determined. These are indicated as grey areas (unknown polarity) in the magnetostratigraphy (figures 9 and 10).

However in most cases, the overprint component is not completely removed at 200 degrees. It was further removed along with the original component. This makes clear interpretation of ChRM unable. In most of these cases, we are still able to determine a normal or reversed polarity by looking at the demagnetization diagrams in combination with equal area projection. If a ChRM component is of a normal polarity, it lies in about the same direction as the present day field overprint. In equal area projection, this would produce a data cloud in the north part (e.g. figure 8, samples CR32-02 and VT 080). In the case of a ChRM of reversed polarity, there is somewhat of a path visible. The two components create a plane, of which the trace is visible in equal area projection (e.g. figure 8, samples CR51-01 and VT063).

Based on the interpretation of the demagnetization diagrams, we find a somewhat large number of reversals. In addition, uncertainty of polarity and large differences in sedimentation rate (based on lithology) makes correlation to the polarity timescale of Lourens et al. (2004) difficult.

5. Discussion

5.1 Nature of the Viqueque Basin

The Viqueque Fm. lies unconformable on top of the Bobonaro tectonic mélange. This implies that the Viqueque Fm. was deposited after an initial tectonic phase. In East Timor, the Cretaceous to Lower Cenozoic part of the stratigraphy, known as the Kolbano Fm., is missing. The Kolbano Fm. lay on top of the Jurassic Wailuli Fm., a formation which mainly consists of scaly clay which is mechanically very weak (Harris et al., 1998). Charlton et al. (1991) have identified the Kolbano Fm. in seismic reflections from the Timor Sea, south of the island. A submarine fold and thrust belt was identified with a southward movement sense of the thrusts. This is overlain by younger sediments, which are possibly the time-equivalent of the Viqueque Fm. (see figure 13). In the West of Timor, the Kolbano Fm. is found in the form a fold and thrust belt.

We hypothesize that the Kolbano Fm. became gravitationally unstable during the initial tectonic phase, and have slid off the Wailuli Fm. Due to its weak mechanical properties this sliding can happen at low angles. To achieve this, there must have been an initial build up of topography. There are a two of processes which can be the cause: 1) stacking of the Cribas and Aitutu units, 2) due to mud diapirism resulting from the emplacement (exhumation) of the tectonic mélange. However mud diapirism can also be the result of pressurized water in between clay. It is likely that the initial build up of topography is the result of a combination of these processes.

The exhumation of the tectonic mélange is the result of Wailuli Fm. becoming the upper decollemant. In a sense, this horizon becomes a subduction channel. The exhumed Wailuli Fm. clays incorporate blocks forming the Bobonaro mélange. Since the Viqueque Fm. lies on top of the Bobonaro mélange, it must be younger than the exhumation of the mélange. The base of the Viqueque Fm. thus gives an minimum age for when the Wailuli Fm. became the upper decollemant. The age of the Viqueque Fm. gives an minimum age to when most distal parts of the Australian continental margin was subducted.

5.2 Age model: based on micropaleontology

Haig and McCartain (2007) have worked on the Viqueque Type section. Therefore we can use their interpretations to create an age model. Haig and McCartain (2007) have found the base of the VT-section to be in the N18/N19 foraminifera zone, indicating an age of the base >4.2 Ma. They infer the base of the section between 5.6 and 5.2 Ma based on FO *Globorotalia tumida* and absence of *Sphaeroidinella dehiscens.* They find at 35m: 3.35 Ma and at 180m: 3.12 Ma, thus here is a minimum of 2.08 Myr in the section.

We find, for the same section, an age near the base of 4.35 at 10m (FO *Globorotalia crassaformis*). We have found *Globorotalia tumida* throughout the section, and the first occurrence of *Sphaeroidinella dehiscens* about 12m from the base of the section. Thus we can only say that the base of the section is younger than 5.57 Ma and older than 5.53 Ma (FO *Globorotalia tumida* (pacific), FO *Spaeroidinella dehiscens*, all ages based on Wade et al., 2011). However the absence of a species within a sample could also be due to poor preservation. Then an age range for the base of the section would be between 5.57 and 4.35 Ma.

The occurrence of *Globorotalia crassaformis*, *Dentoglobigerina altispira*, and *Globoturborotalita obliquus* combined with the absence of *Globorotalia tosaensis* and *Globigerinoides fistulosis* throughout the stratigraphy suggests that the top has to be older than 3.47 Ma (LO *Dentoglobigerina altispira* (pacific)), ages from Wade et al. (2011). This would give a minimum of

0.88 Myr in the section (using 4.35 Ma for the base). Using the 5.57Ma for the base, there would be a minimum of 2.10 Myr present in the section.

5.3 Age model: based on magnetostratigraphy

In both sections we find a number of reversals. This allows us to correlate with the polarity timescale of Lourens (2004). However, we have to assume that all ChRM directions are primary directions. This is not necessarily the case. During deposition of Viqueque Fm. Timor was at similar latitude as today. Thus the overprint of the present day field has somewhat the same direction as normal ChRM directions. In addition, samples with a very weak reversed ChRM signal can be completely overprinted by the present day field, and be interpreted as a normal ChRM direction.

Another problem with the interpretation of samples arises from secondary, post-diagenetic greigite. Vasilev et al. (2008) showed that bacteria form greigite strains. These hold magnetization preferently in the direction of the then present field. Sample levels which were deposited near or during a reversal, can thus show both a normal and reversed component.

Correlation to the polarity timescale is not straightforward. However, based on the pattern and taking variable sedimentation rates (generally higher more up in the stratigraphy) we can make a correlation. For the Viqueque Type Section we find ages of 5.235 Ma at 24m (base of chron C3n.4n), a number of reversals in between up to 2.581Ma (base of chron C2r.2r) at 187m. Based on this we find a minimum of 1.719 Myr in the section., see figure 9 For the Caiaco River Section we find ages of 4.493 Ma at 35m (base of chron C3n.1r), a number of reversals in between up to 1.945 Ma at 480m (base of chron C2n). Based on this interpretation we find a minimum of 2.548 Myr in the section.

It can be observed that the biostratigraphy and the magnetostratigraphy are not in agreement. As discussed, the correlation to the polarity timescale of Lourens et al. (2004) is not necessarily correct. For instance if a sample is interpreted as having a normal ChRM polarity, it could also be that the ChRM initially was reversed, but became completely overprinted. If this is the case for a number of stratigraphically consecutive samples, two reversals are identified which never happened.

5.4 Scenarios for sedimentation- and uplift rates

Based on the tectonostratigraphy we can infer that the section is of Late Miocene to Pliocene age. But further age determination is difficult. This study and that of Haig and McCartain (2007) somewhat agree on the age of the base. Both studies indicate there is a very low sedimentation rate at the base: >4mm/kyr (Haig &McCartain, 2007); >8.2mm/kyr (this study). The sedimentation rate (from about 10m in the section) goes up considerably; 621.7 mm/kyr (Haig & McCartain (2007), from 35m to 178m in 0.23 Myr); >261.4 mm/kyr (this study, from 10m to 240m in 0.88 Myr). This change to higher sedimentation rates can be explained by parts of Timor emerging and being eroded. This coincides well with the first debris flow, present in the section at 50m from the base, which shows rounded pebbles.

Uplift rates can be calculated using the depth indications from benthic foraminifera. Haig & McCartain (2007) documented lower to middle bathyal (depth range of 3-1 km) up to 3.35 Ma, and upper middle bathyal (depth range not published, assumed at 1-0.2 km) at <3.12 Ma. This gives a range of uplift rates from 0 to 12.2 mm/yr (using a dept difference of 0 to 2.8 km in 0.23 Myr). Such a high uplift rate seems unlikely. It would imply the basin has gone up from 3 km to

0.2 km depth within 0.23 Myr. Further constraints on paleodepth are necessary for further interpretations.

Our study indicates a similar, shallowing trend. Lower to middle bathyal (<750 m) at 4.35 Ma to upper to middle bathyal (350 to 750 m) at <3.47Ma. Our uplift rates range from 0 to >0.454 mm/yr (0 to 400 m depth difference in 0.88 Myr). If we assume maximum depth of 3 km for the lower-middle bathyal zone we find a maximum uplift rate of 3.01mm/yr. This interpretation is based on the biostratigraphy alone. If we use ages derived from interpreted magnetostratigraphy we arrive at uplift rates which lie within the ranges derived from biostratigraphy. For further discussion we will work with this range.

5.5 Uplift from stacking of the sediments.

We apply a simple model to explain the uplift based on isostasy. Isostasy can be seen as the principle of buoyancy or Archemidis' principle, applied to geological problems. For example: a plank of wood is floating on top of water. This single plank has half its thickness submerged, half above the water level. If we add another plank on top of this initial one, the first plank is completely submerged, while the second plank is above water. This represents a thickening of 2, resulting in half a plank's thickness in added height with respect to the water level. This example demonstrates Airy-type isostasy. Topography is accommodated by changes in thickness, and densities are constant.

We can use this principle on a geological scale. We can use the thickening factor from Tate et al. (2011) to explain the uplift. We assume that only the sedimentary succession (Aitutu and Cribas formations) is homogenously thickened (see figure 3, from Tate et al. (2011)). The underlying basement is unaffected. Thickening of the sediments pushes down the basement, as well as building topography. This results in the following equation (for derivation, see appendix):

$$h = \frac{t_s(\beta - 1)(\rho_s - \rho_m)}{\rho_m - \rho_o} + d \qquad (1)$$

In which, h is the resulting bathymetry (negative values imply topography), t_s is the thickness of the sedimentary succession, β is the thickening factor, derived from cross section balancing, d the original bathymetry or water depth, ρ density (of subscript: s, sediments; m, mantle; o, oceanic water). For values see table 1. Figure 4 shows the model setup.

Detailed cross section balancing by Tate et al. (2010) (see figure 3) allow us to calculate a range of thickening factors. For the transect "Liquica-Ainaro": 512 km restored and 156 km deformed Australian strata results in a thickening factor of 3.28. For the transect "Dili-Barique": 597 km restored 181 km deformed Australian strata: thickening factor 3.30. If we assume the thickening factor to be 1 at the start of collision (at 5.5 Ma), and a linear increase to 3.3 (e.g. homogeneous thickening, or gradual build up of thickening), we can reconstruct the bathymetry using equation 1 and the values of table 1. The results are shown in figure 14.

With these assumptions, we cannot explain the uplift reflected in the sediments of either the east or west part of Timor. Based on this assumption alone we find an uplift rate of 0.331 mm/yr. Even if we place the start of uplift at 4.35 Ma (youngest estimate based on FO *Globorotalia crassaformis*), we find an uplift rate of 0.418 mm/yr. This model is strongly dependent on the initial water depth. With the results shown in figure 14, an initial water depth of d = 3 km was

used. Using an initial water depth of d = 2 km the whole uplift history would shift 1 km up. It would however not change the uplift rate, since the thickening rate stays the same.

Other studies have focused on the uplift of Timor. Audley-Charles (1986) found uplift rates of 3 mm/yr between 5 and 3 Ma, and 1.5 mm/yr after 3 Ma, based on micropaleontology. These values are much higher than we can explain with stacking. De Smet et al. (1990) worked with chronostratigraphy and paleobathymetry. They found two short rapid uplift rates for sediments younger than 3 Ma. One at ~2 Ma of 2-3 mm/yr (see figure 14), and one at ~0.2 Ma of 5-10 mm/yr. However de Smet et al. use an older timescale, that of Berggren et al. (1985). In addition, the sampled section lies about 200 km west of the Viqueque Type section. It is likely that the same process has been taking place. We do observe the same Pliocene uplift trend. But still the thickening history can be different. We do not know the thickening factor from that transect. The relatively short uplift phases cannot be explained by homogeneous thickening. The low values in between do lie in within the modeled range.

Roosmawati and Harris (2009) have reconstructed the uplift of the islands of Rote and Savu. These islands lie 400 km west from East Timor. But, as with the data from de Smet et al. (1990), we can compare to Roosmawati and Harris' data because similar processes are likely taking place. They find a gradual uplift between 5.2 to 1.7 Ma of 0.5 mm/yr. This is somewhat similar to the uplift rate derived from the model. However, we are not sure if the thickening factor underneath the islands of Rote and Savu is similar to that on the East of Timor.

Other studies have focused on the youngest part (< 1.2 Ma) of the uplift history (Merrits et al., 1998; Cox et al., 2006; Harris et al., 2000). Merrits et al. (1998) have determined the uplift by Uranium-dating of raised coral terraces. This resulted in 0.3-1.5 mm/yr. Cox et al. (2006) found similar values. Harris et al. (2000) determined erosion rates using apetite fission track analysis. This resulted in rates between 2.1-3.0 mm/yr. The nature of this erosion might be due to uplift, but can also be a climatic effect.

5.6 Other causes for uplift

Uplift due to stacking is thus just a part of the whole uplift. Other mechanisms are needed to invoke the observed uplift. First of all it should be noted that the assumption of local isostasy probably doesn't hold. Langhi et al. (2011) have shown that flexure of the bended Australian plate plays a big role in the present day bathymetry in the Timor Sea. This would mean that a part of the load (thickened sediment) is supported by the lithospheric strength. Even though, we can use isostasy as an end member. Flexure can explain higher uplift rates since the basement is not isostatically subsiding (e.g. sinking less than expected assuming isostasy), but stays somewhat on the same level. Using this end member (no subsidence of the basement) the uplift would be in perfect correlation with the thickening factor. For example, with the emplacement of 1 duplex (thickening factor: 2) the resulting bathymetry would be 2 km shallower (using an initial sediment thickness of 2 km). But even with the most ridged plate (the flexure end-member situation). This would not explain the sudden increase we find in the uplift history.

The same problem arises when we try to explain the uplift with dynamic topography. Dynamic topography is the result of mantle flow underneath the studied system. However, typical mantle flow induced vertical motions are much slower than the uplift rates we find. The sediments reflect a rapid phase of uplift. There are a couple of mechanisms which can cause this: activation of a thrust, slab breakoff and delamination.

The Wetar thrust (North of Timor) could have become active and take up the uplift. In this scenario the whole of Timor would be pushed up as a large piggy-back basin. However than we would not expect a deep (3 km, Audley-Charles (2004)) basin between Wetar and Timor (Wetar Strait), unless the initial depth between Timor and Wetar was very deep. In addition the Wetar thrust itself is a shallow lying fault. If it lies at a 30° dip angle, then for every meter of uplift, there must have been two meters of fault displacement. The amount of uplift can be taken up by the Wetar thrust, even if it has a shallower dip angle. An uplift of 400 m would be caused by 800 m fault displacement (assuming a 30° dip angle). This reflects in 692 m horizontal movement. If it does this in the 0.88 Myr the Wetar thrust should accommodate relative plate speed of 0.78 mm/yr. Recent plate speeds (Asia-Australia) are in the range of centimeters per year (Nugroho et al., 2009). If this plate speed can be translated to 5.5 Ma, then the associated uplift rate would be much too high. However in principle the Wetar thrust can explain gradual uplift if the fault was much less active in the past. Nugroho et al. (2009) have also shown that the relative speed between Wetar and Timor is very low. This makes the piggy-back basin hypothesis more plausible. But to test the hypothesis we need to know how much movement there was in Wetar throughout the late Miocene and Pliocene and see if the irregular changes in uplift rates coincide with changes in fault sliprate.

Slab breakoff is a process which can cause a rapid phase of uplift (e.g. van der Meulen et al., 2000; Zachariasse et al., 2008; Andrews and Billen, 2009). However there are different ways in which the slab can break off. Zachariasse et al. (2008) investigated slab breakoff in a STEP (Subduction Transform Edge Propagator, Govers and Wortel, 2005) situation in Greece. They found an uplift of 500-700m between 5 and 3Ma. This implies a maximum uplift of 0.35 mm/yr. This number might not be representative due to large fluctuations in sea level in the Mediterranean. van der Meulen et al. (2000) have studied uplift rates in a setting where the slab is tearing off laterally, namely the Apenninic foredeep, Italy. They have found minimum uplift rates of 1.62 mm/yr. Numerical modeling studies have attempted to find uplift rates associated with slab breakoff. Uplift rates vary depending on the initial setup of the model. Andrews and Billen (2009) have found uplift rates to range between 0.39 and 2.65 mm/yr for regular 2D slab breakoff. Their results show a total uplift of >5km can occur in less than 5 Myr. Slab breakoff could create the pulse of uplift like we see in Timor.

Slab breakoff was initially proposed by Audley-Charles (1986). Following his work, Keep and Haig (2010) have proposed slab breakoff between 4.5 and 3.1 Ma. They argue that between 5.5 and 4.5 Ma subduction was locked which caused a tectonic quiet interval coinciding with the low uplift rate in this interval. However seismic tomography (e.g. Spakman and Hall, 2010) does not show a clear detached slab. Instead, the slab underneath Timor can be continued all the way to the Australian continental shelf. Sandiford (2008) also finds that the slab is intact, but rupturing due to down dip extension of the slab. In other words, the slab is necking, about to break thus hasn't broken off yet.

If detachment is not an option, another cause could be found in the process of delamination. Spakman and Hall (2010) hypothesize that the Australian slab is stuck with reference to the mantle, and that the Australian plate is continuing its northward movement. If so, Timor is still being pushed northward. If the slab stays behind in the south, Timor's upper crust has to detach from the lithosphere. This is hypothesized by Audley-Charles (2004), and by Spakman and Hall (2010). They argue that the depression in the Timor Sea is caused by downpulling of the slab.

Thus, the slab is not present under Timor. Tomographic studies currently do not have the resolution to resolve this question.

Valera et al., 2011 have shown, using a numerical model, that delamination is possible. At the moment, no studies have been published which attempt to find out what uplift rates delamination would produce. But even without numbers, qualitatively we can say that, if the root is removed and replaced by asthenospheric material (which has a lower density) this will cause uplift. Additional uplift could be created by the unbending of the upper crust (assuming delamination at the boundary of upper to lower crust). For the time being, this seems to be the best option to explain the uplift history of Timor.'

6. Conclusion

This paper set out to investigate the relation between crustal thickening and uplift. We test the hypothesis that the uplift of Timor can be explained isostatic effects due to the emplacement of a fold-and-thrust belt. To this end, we have reconstructed the uplift history based on bio- and magnetostratigraphy of a syn-orogenic basin. We compare our results with the theoretical uplift we would expect due to thickening of the fold-and-thrustbelt, using thickening factors derived from balanced sections (Tate et al., 2010).

Both Haig & McCartain and this study find a low uplift rate in the basal part, followed in an increase in both sedimentation rate and uplift. Uplift rates range from 0 to 3.01 mm/yr. Theoretical uplift would be about 0.5 mm/yr. Thickening of the fold-and-thrust belt on Timor can thus only explain a part of the uplift history.

Both Haig & McCartain (2007) and this study find a shift in uplift rate. Three mechanisms are proposed for the shift to rapid uplift. Activation of the Wetar thrust could explain the uplift but is poorly constrained. Slab detachment has been proposed, but this isn't likely due to the lack of evidence from seismic and tomographic studies. Delamination is a preferred mechanism to explain Timor's uplift history. From ~5.5 to 4.35 Ma the uplift can be explained by stacking of Australian continental shelf sediments. After 4.35 Ma, the upper crust starts to delaminate from the Australian lithosphere, causing a pulse of uplift, shifting southward with respect to Timor.

To resolve the question on what caused the uplift in Timor, we need a better age model for the Viqueque Fm. This could possibly be achieved by tuning to an astronomical solution (e.g. Lourens et al., 2004) of the lower part of the stratigraphy. Possible tuffs or other volcanics-related ashes could be dated using Ar/Ar methods. This would result in accurate tie-points. For the magnetostratigraphy we mainly used shales. Perhaps other lithologies provide better ChRM directions. More certainty on reversals can also be achieved by measuring the 2nd sample (two samples per sample level), and/or by improving the sample resolution. Improving the sample resolution for biostratigraphy would improve the identification of FO or LO's in the section.

But, perhaps more important are the controls on depth. The uplift rates in this study have a large range due to the uncertainty of deposition depths. Now these are based on a sparse number of benthic foraminifera within the samples. Perhaps larger quantities of the samples can be washed and prepared to improve the chances of finding benthic foraminifera.

Acknowledgements

I'd like to thank Douwe van Hinsbergen for granting me the opportunity to work on the "Australia Down Under" project. He was, along with Nadine McQuarrie, Ron Harris, Garrett Tate

and Brendan Duffy so kind to help me out in the field with insightful discussions. Mario Amaral and Jhonny Suarez da Costa are thanked for their help translating and explaining to the local people what (the hell) we were doing in their rivers, and perhaps most of all with the work collecting samples, if not for the conversations about missing our girlfriends when drinking beers after a day in the field. The paleomagnetic work could not have been carried out if not for the help of the people at Fort Hoofddijk Paleomagnetic Laboratory in Utrecht. Especially Tom Mullender, Iuliana Vasiliev, Silja Huesing and Cor Langereis are thanked for helping me out whenever I dropped in with a question and Wout Krijgsman for starting me up. Jan Willem Zachariasse and Geert Itmann are thanked for their extensive help with the biostratigraphy. Douwe van Hinsbergen and Inge Loes ten Kate supplied me with plenty of comments to improve the initial version of this thesis.

References

Andrews, E.R., Billen, M.I., 2009. Rheologic controls on the dynamics of slab detachment. Tectonophysics , vol. 464, pp. 60–69.

Audley-Charles, M.G., 1967. Greywackes with a primary matrix from the Viqueque Formation (Upper Miocene-Pliocene), Timor. Journal of Sedimentary Petrology, vol. 37, no.1 pp 5-11.

Audley-Charles, M.G., 1968. The Geology of Portugeuse Timor. Memoirs of the Geological Society, Londen. Vol.4, pages 1-76

Audley-Charles, M.G., 1986. Rates of Neogene and Quaternary tectonic movements in the Southern Banda Arc based on micropaleontology. Journal of the Geological Society, vol. 143, pp. 161-175

Audley-Charles, M.G., 2004. Ocean trench blocked and obliterated by Banda forearc collision with Australian proximal continental slope. Tectonophysics, vol. 389, pp. 65–79.

Ayarza, P., Alvarez-Lobato, F., Teixell, A., Arboleya, M.L., Tesón, E., Julivert, M., Charroud, M., 2005. Crustal structure under the central High Atlas Mountains (Morocco) from geological and gravity data. Tectonophysics, vol. 400, pp 67-84.

van Bemmelen, R.W., 1949. The Geology of Indonesia, IA. Government Printing Office, The Hague, Netherlands, pp. 732.

Braun, J., 2010. The many surface expressions of mantle dynamics. Nature Geosciences, vol.3 pp 825-833.

Berggren, W. A, Kent, D. V. and Van Couvermg, J A. 1985. The Neogene: part 2, Neogene geochronology and chronostratigraphy. In: The Chronology of the Geological Record (Edited by Snelling, N. J.). Geol Soc Lond. Mere 10, pp. 211-260.

Burov, E.V., Kogan, M.G., Lyon-Cean, H., Molnar, P., 1990. Gravity anomalies, the deep structure and dynamic processes benieat the Tien Shan. Earth and Planetary Science Letters, vol. 95, pp 367-383.

Cox, N.L., Harris R.A., and Merritts, D., 2006. Quaternary Uplift of coral terraces from active flooding and thrusting along the Northern Coast of Timor-Leste, American Geophysical Union Abstract 87 (52).

Charlton, T.R., Barber, A.J. and Barkham, S.T., 1991. The structural evolution of the Timor collision complex, eastern Indonesia, Journal of Structural Geology, vol. 13, pp. 489-500.

Earle, M.M., 1981. The metamorphic rocks of Boi, Timor, eastern Indonesia. In: Barber, A.J., Wiryosujono, S. (Eds.), The Geology and Tectonics of Eastern Indonesia. GRDC Spec. Pub., vol. 2, pp. 239–251.

Govers, R., Wortel, M.J.R., 2005. Lithosphere tearing at STEP faults: response to edges of

subduction zones. Earth Planetary Science Letters, vol. 236, pp. 505–523.

Haig, D. W. and McCartain, E., 2007. Carbonate pelagites in the post-Gondwana succession (Cretaceous - Neogene) of East Timor. Australian Journal of Earth Sciences, vol. 54: 6, pp 875-897.

Harris, R.A., Sawyer, R.K. and Audley-Charles, M.G., 1998. Collisional melange development: Geologic associations of active melange forming processes with exhumed melange facies in the western Banda orogen, Indonesia. Tectonics, vol. 17, pp. 458-480.

Harris, R. A., Kaiser, J., Hurford A. and Carter, A. 2000. Thermal history of Australian passive margin cover sequences accreted to Timor during Late Neogene arc – continent collision, Indonesia. Journal of Asian Earth Sciences, vol. 18, pp. 47 – 69

Harris, R.A., 2006. Rise and fall of the Eastern Great Indonesian arc recorded by the assembly, dispersion and accretion of the Banda Terrane, Timor. Gondwana Research, vol. 10 pages 207–231.

van Hinsbergen, D.J.J., Kouwenhoven, T.J. and van der Zwaan, G.J., 2005 Palaeobathymetry in the backstripping procedure: correction for oxygenation effects on depth estimates. Palaeogeography, Palaeoclimatology, Palaeoecology, vol. 221(3-4), pp. 245-265.

Keep, M., and Haig, D.W., 2010. Deformation and exhumation in Timor: Distinct stages of a young orogeny. Tectonophysics, vol. 483, pp. 93–111.

Krs, M., Novak, F., Krsova, M., Pruner, P., Koulíková, L. and Jansa, J., 1992. Magnetic properties and metastability of greigite-smythite mineralization in brown-coal basins of the Krusné hory Piedmont, Bohemia. Physics of Earth and Planetary Interior, vol. 70, pp. 273–287.

Langhi, L., Ciftci, N.B., Borel, G.D., 2011. Impact of lithospheric flexure on the evolution of shallow faults in the Timor foreland system. Marine Geology, vol. 284, pp. 40–54

Lourens, L.J., Hilgen, F.J., Shackleton, N.J., Laskar, J., Wilson, D., 2004. The Neogene Period. In: Gradstein, F.M., Ogg, J.G., Smith, A.G. (Eds.), Geological Time Scale 2004. Cambridge University Press, pp. 409–440.

van Marle, L.J., 1989. Late Cenozoic palaeobathymetry and geohistory analysis of Central West Timor, eastern Indonesia. Marine and Petroleum Geology, vol 8, pp. 22-34.

Merritts, D., Eby, R., Harris, R.A., Edwards, R.L., Chang, H., 1998. Variable rates of Late Quaternary surface uplift along the Banda Arc–Australian plate collision zone, eastern Indonesia. In: Steward, I.S., Vita-Finzi, C. (Eds.), Coastal Tectonics. Special Publication, vol. 146. Geological Society, London, pp. 213–224.

van der Meulen, M.J., Buiter, S.J.H., Meulenkamp, J.E., and Wortel, M.J.R., 2000. An early Pliocene uplift of the central Apenninic foredeep and its geodynamic significance. Tectonics, vol. 19, pp. 300-313

Molengraaff, G. A. F., 1912. On recent crustal movements on the Island of Timor and their bearing on geological history of the East Indian Archipelago. Proc. Kon. Akad. V. Wetensch. Amsterdam 15, 224–225.

Nugroho, H., Harris, R.A., Lestariya, A.W. and Maruf, B., 2009. Plate boundary reorganization in the active Banda Arc-continent collision: Insights from new GPS measurements. Tectonophysics, vol.479, pp 52-65.

Roosmawati, N. and Harris, R.A., 2005. Surface uplift history of the indipient Banda arc-continent collision: Geology and synorogenic foraminifera of Rote and Savu Islands, Indonesia. Tectonophysics vol. 479, pp 95-110.

Sandiford, M., 2008. Seismic moment release during slab rupture beneath the Banda Sea. Geophysical Journal International, vol. 176, pp. 659-671.

Skinner, B.J., Erd, R.C. & Grimaldi, F.S., 1964. Greigite, the thiospinel of iron; a new mineral. American Mineralogist, vol. 49, pp. 543–555.

de Smet, M.E.M., Fortuin, A.R., Troelstra, S.R., van Marle, L.J., Karmini, M., Tjokrosapoetro, S., Hadiwasastra, S., 1990. Journal of Southeast Asian Earth Sciences, Vol 4, No 4, pp. 337-356.

Spakman, W. & Hall, R. 2010. Surface deformation and slab-mantle interaction during Banda arc subduction rollback. Nature Geoscience, vol. 3,pp. 562–566.

Tate, G., McQuarrie, N, Bakker, R.R., van Hinsbergen, D.J.J., and Harris, R.A. 2010. Active Arc-Continent Accretion in Timor-Leste: New Structural mapping and quantification of Continental Subduction. Abstract T51A1996T presented at 2010 Fall Meeting, AGU, San Francisco, Calif., 13-17 Dec.

Valera, J.L., Negredo, A.M., Jiménez-Munt,I., 2011. Deep and near-surface consequences of root removal by asymmetric continental delamination. Tectonophysics, vol. 502, pp. 257-265.

Vasiliev, I., Franke, C., Meeldijk, J.D., Dekkers, M.J., Langereis, C.G. and Krijgsman, W., 2008. Putative greigite magnetofossils from the Pliocene epoch, Nature Geoscience, Vol. 1, pp 782–786.

Wade, BS; Pearson, PN; Berggren, WA; Paelike, H (2011) Review and revision of Cenozoic tropical planktonic foraminiferal biostratigraphy and calibration to the geomagnetic polarity and astronomical time scale, Earth Science Reviews, 104, pp.111-142

Zachariasse, W.J., van Hinsbergen, D.J.J., Fortuin, A.R., 2008. Mass wasting and uplift on Crete and Karpathos (Greece) during the early Pliocene related to beginning of south Aegean left-lateral, strike slip tectonics. Geological Society of America Bulletin vol. 120, pp. 976–993.

Zeyen, H., Ayarza, P., Fernandez, M., Rimi, A., 2005. Lithosperic structure under the western African-European plate boundary: A transect across the Atlas Mountains and the Gulf of Cadiz. Tectonics, vol. 24, pp 1-16.

Zijderveld, J.D.A.,1967. A.C. demagnetization of rocks: analysis of results. In: Runcon, S.K. (Ed.), Developments in Solid Earth Geosciences Methods in Paleomagnetism. Elsevier Publishing Company, Amsterdam.

Figures Caption

Figure 1. Tectonic setting.

Figure 2A. East Timor locality map with locality of Viqueque Fm. and sampling locations indicated. After Haig & McCartain, (2007).

Figure 2B. Sampling locations with aerial photographs.

Figure 3. Cross section balancing for Central Timor. From Tate et al. (2011)

Figure 4. Model setup. Left column shows reference (undeformed) state. Right column deformed state. Abbreviations: m, mantle; c, crust; ts, sediments; d, original bathymetry; h resulting bathymetry.

Figure 5. Detailed Lithostratigraphic log of the Viqueque Formation at the town of Viqueque, (VT-section). With sample levels indicated.

Figure 6. Detailed Lithostratigraphic log of the Viqueque Formation at Caiaco River (CR-section). With sample levels indicated.

Figure 7. Thermomagnetic run in air for a representative sample (shale lithology)

Figure 8. Representative demagnetization diagrams for samples from CR and VT sections. From top to bottom four samples are shown, 2 from each section; CR32-02 (normal), CR51-01 (reversed), VT063 (reversed) and VT080 (normal). For each sample, left panel: Zijderveld diagram without tectonic correction (shows overprint of present day field), middle panel: Zijderveld (1967) diagram with tectonic correction, right panel: equal area projection. For uses see text.

Figure 9. Magnetostratigraphy with simplified lithostratigraphy for CR-section. Black indicates Normal polarity, white reversed, grayscales uncertain polarity.

Figure 10. Magnetostratigraphy with simplified lithostratigraphy for VT section. Black indicates Normal polarity, white reversed, grayscales uncertain polarity.

Figure 11. Planktonic foraminifera found in the Viqueque Type Section (VT). Key: 1: *Dentoglobigerina altispira*;2: *Globorotalia menardii*; 3: *Globorotalia tumida*; 4: *Dutertrei humerosa*; 5: *Sphaeroidinellopsis*; 6: *Pulleniatina primaris*; 7: *Pulleniatina preacursor*; 8: *Globorotalia crassaformis*; 9: *Sphaeroidinella dehiscens*; 10: *Globorotalia scitula*; 11: *Globorotalia ruber*; 12: *Globigerinoides conglobatus*; 13: *Sphaeroidinellopsis seminula*; 14: *Globoturborotalita obliquus*; 15: *Globigerina rubescens*.

Figure 12. Benthic foraminifera found in the Viqueque Type Section (VT). Key: 1: *Oridorsalis*; 2: *Cibicides bradyi*; 3: *Siphonina*; 4: *Cibicides wuellersorfi* (flat); 5: *Karreriella*; 6: *Cibicides wuellerstorfi*; 7: *Cibicides (-)*; 8: *Globocassidulina*; 9: *Sigmoilopis*; 10: *Gyroidina*; 11: *Nonion pompiloides*; 12: *Laticarina*; 13: *Lagena*; 14: *Pullenia*; 15: *Sphaeroidina*; 16: *Uvigerina*; 17: *Eponides*; 18: *Amphistegina*; 19: *Elphidium*; 20: *Heterolepa*; 21: *Stilstomella*; 22: *Bulimina*; 23: *Cibicides ungarianus*.

Figure 13. Illustration to the tectonostratigraphic relations. Cross section view North (left) to South (right).

Figure 14. Uplift trough time from 5.5Ma to present day shown: model results, results from Haig & McCartain (2007), this study (Both VT-section, East Timor) and de Smet et al. (1990) (West Timor). It should be pointed out that de Smet et al., use an older timescale, that of Berggren et al. (1985).

Tables Caption

Table 1. Used variables and their values

Figures

Figure 1.

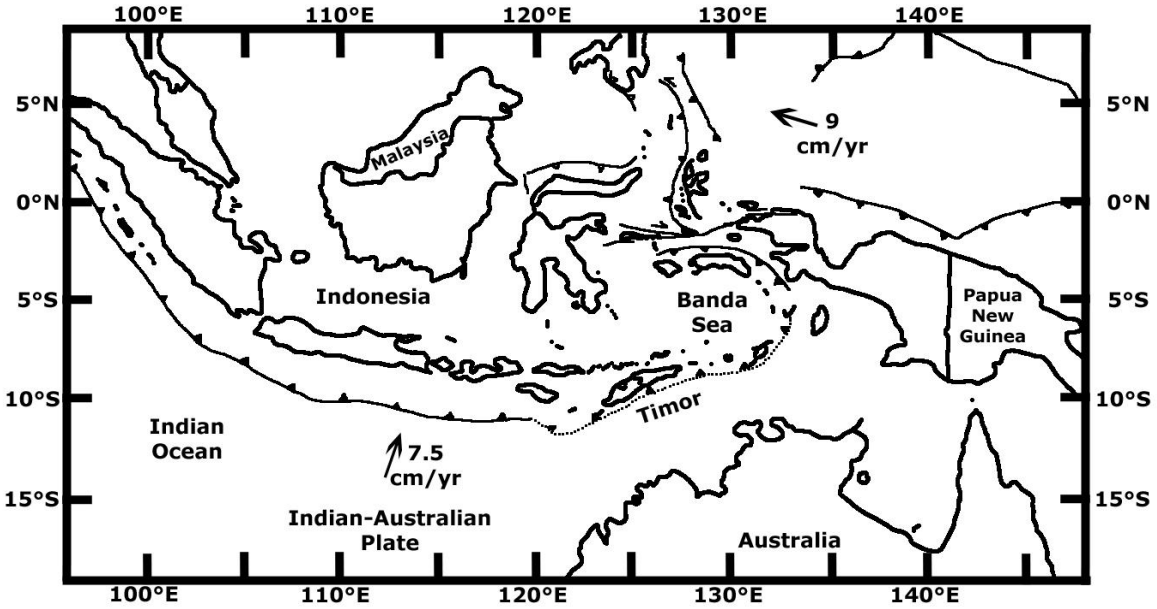

Figure 2a.

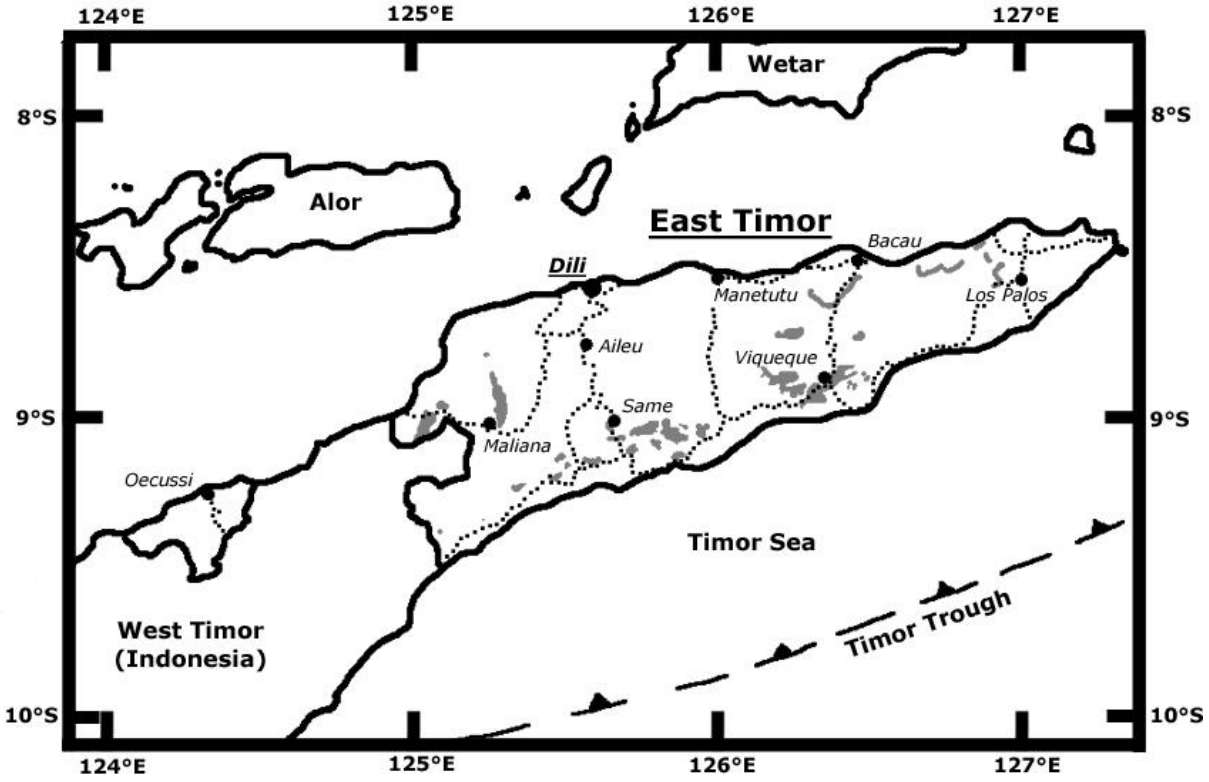

Figure 2B.

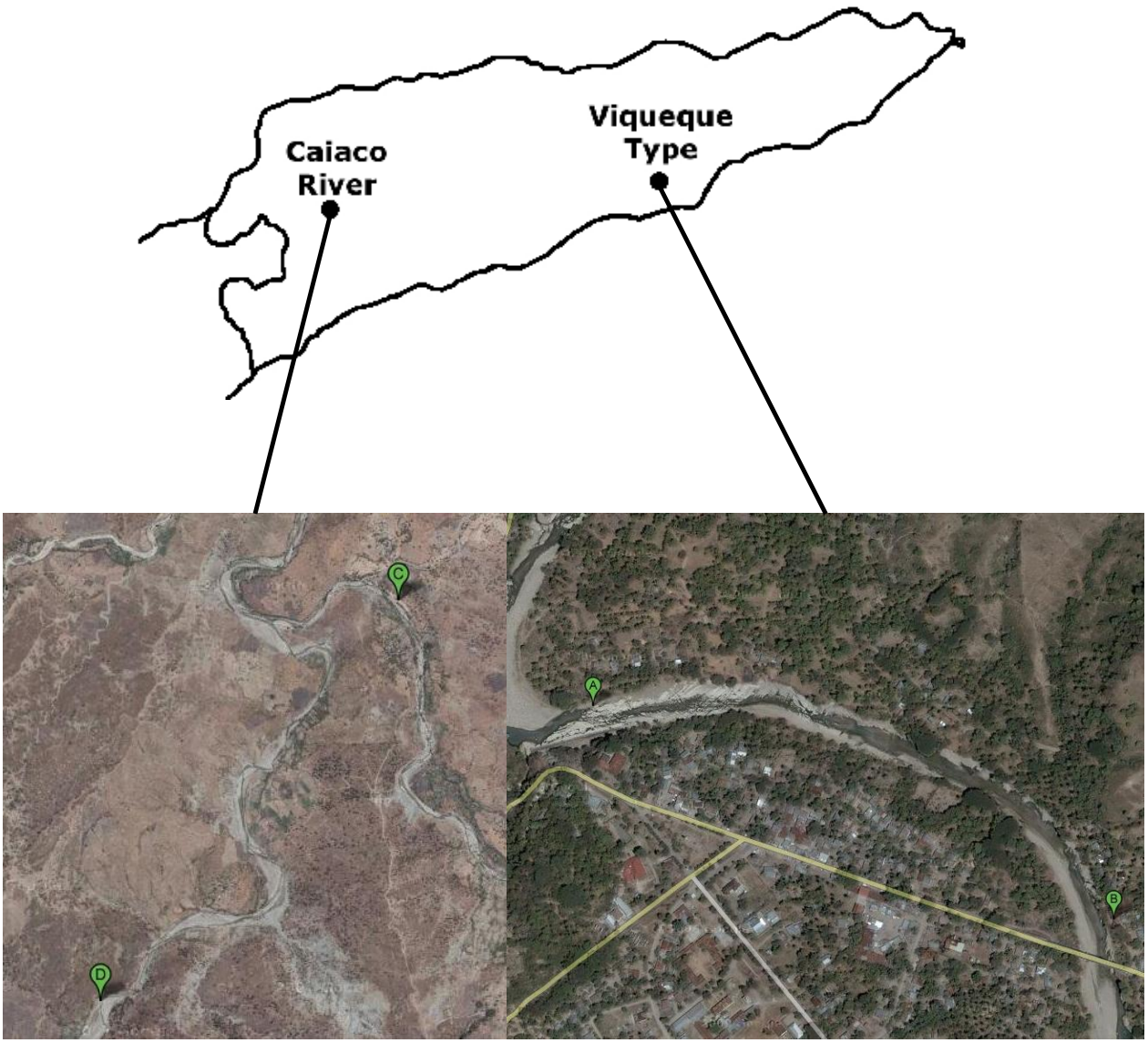

Figure 3.

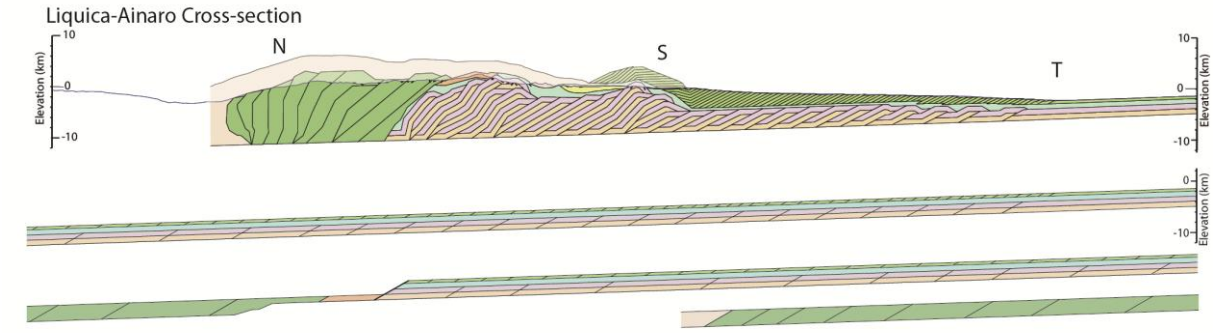

Figure 4.

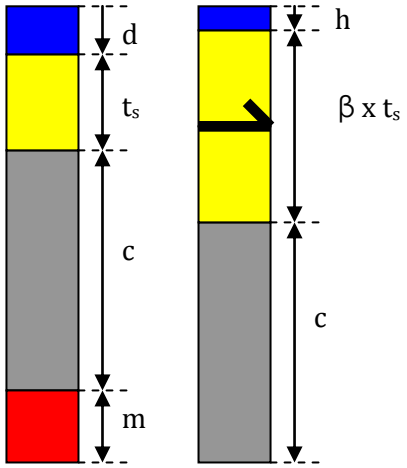

Figure 5.

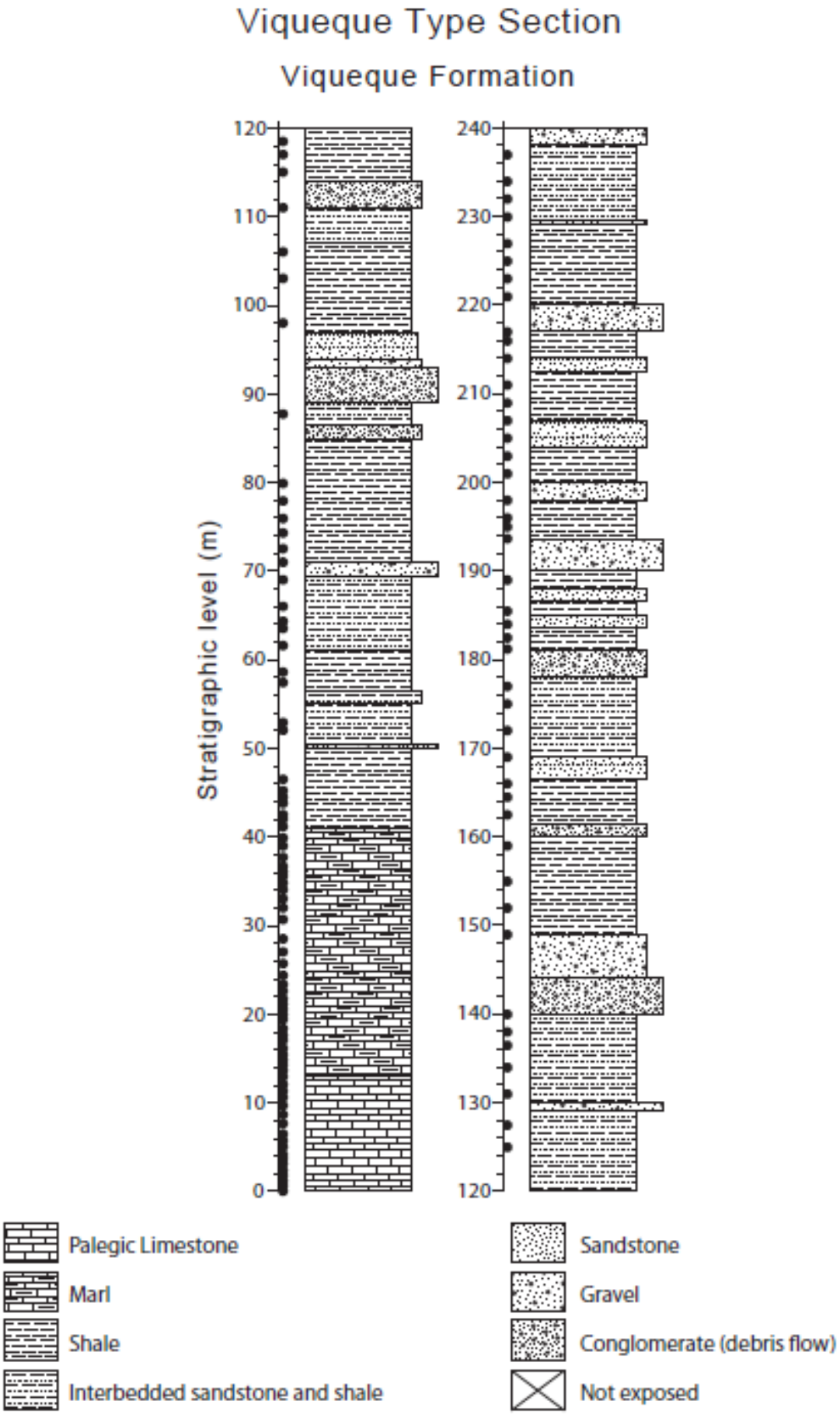
Viqueque Type Section
Viqueque Formation
Stratigraphic level (m)
0
10
20
30
40
50
60
70
80
90
100
110
120
120
130
140
150
160
170
180
190
200
210
220
230
240
Palegic Limestone
Marl
Shale
Interbedded sandstone and shale
Sandstone
Gravel
Conglomerate (debris flow)
Not exposed

Figure 6.

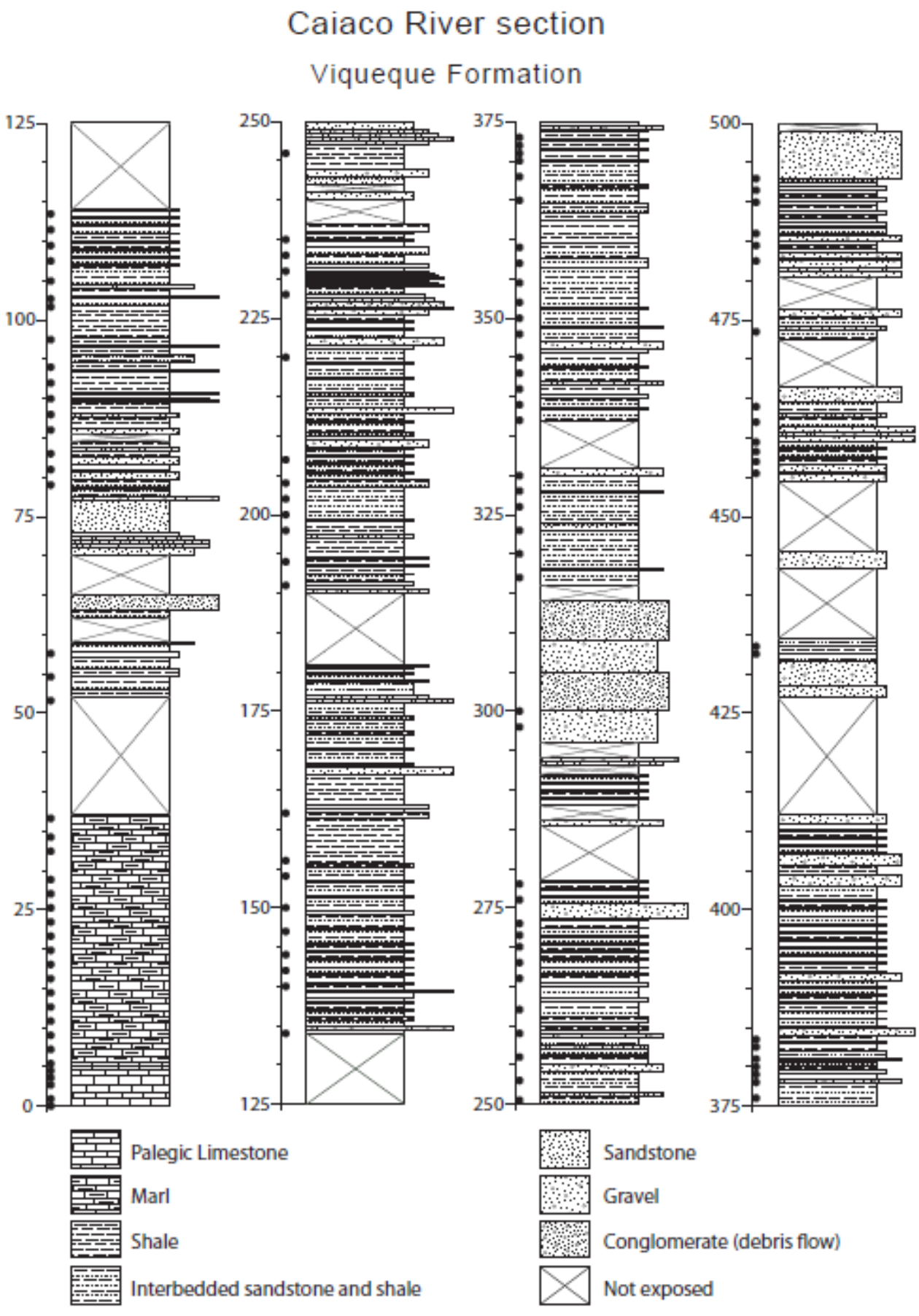
Caiaco River section
Viqueque Formation
125
100
75
50
25
0
250
225
200
175
150
125
375
350
325
300
275
250
500
475
450
425
400
375
Palegic Limestone
Marl
Shale
Interbedded sandstone and shale
Sandstone
Gravel
Conglomerate (debris flow)
Not exposed

Figure 7.

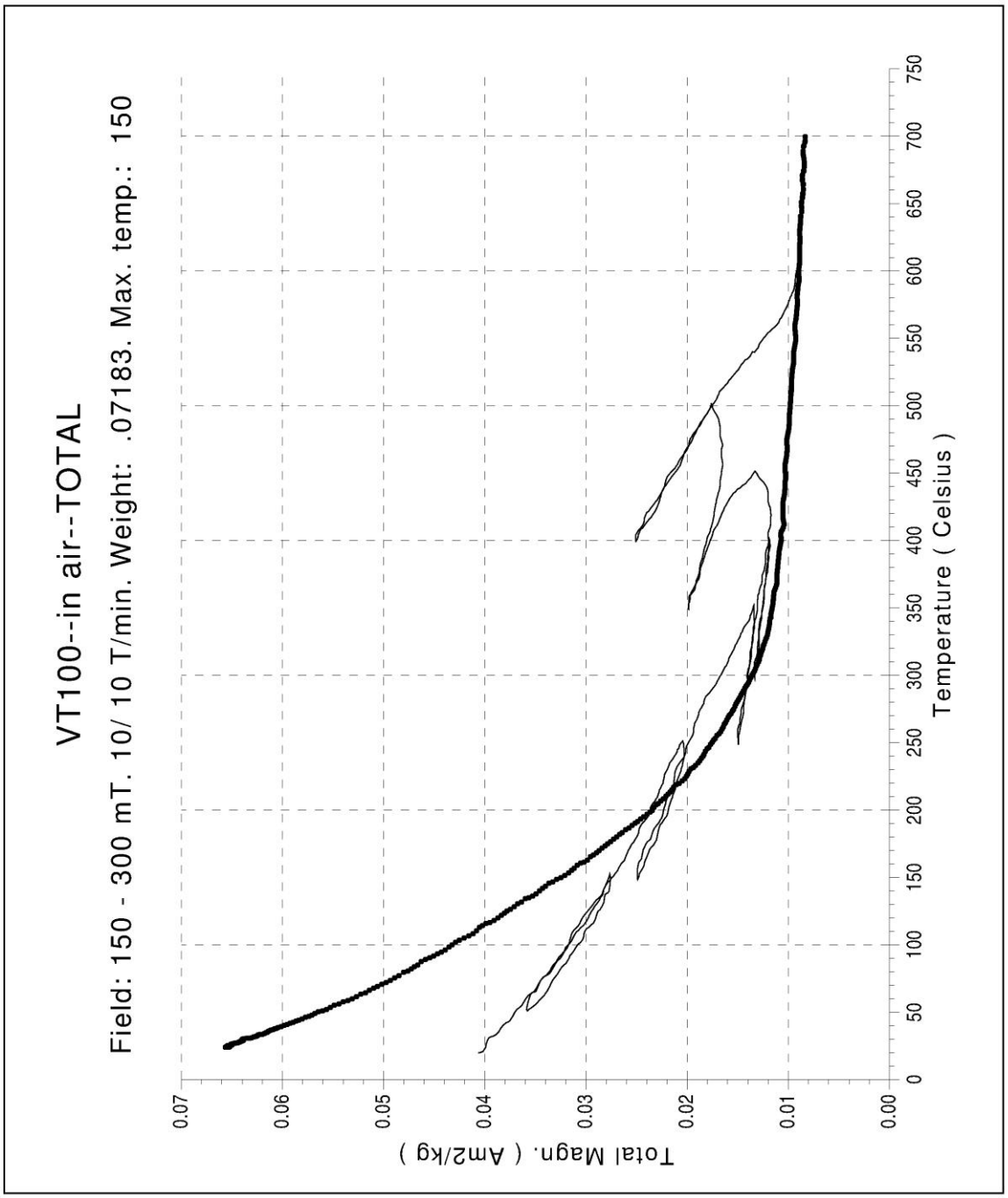
VT100--in air--TOTAL
Field: 150 - 300 mT. 10/ 10 T/min. Weight: .07183. Max. temp.: 150
Total Magn. (Am2/kg)
0.07
0.06
0.05
0.04
0.03
0.02
0.01
0.00
0
50
100
150
200
250
300
350
400
450
500
550
600
650
700
750
Temperature (Celsius)

Figure 8.

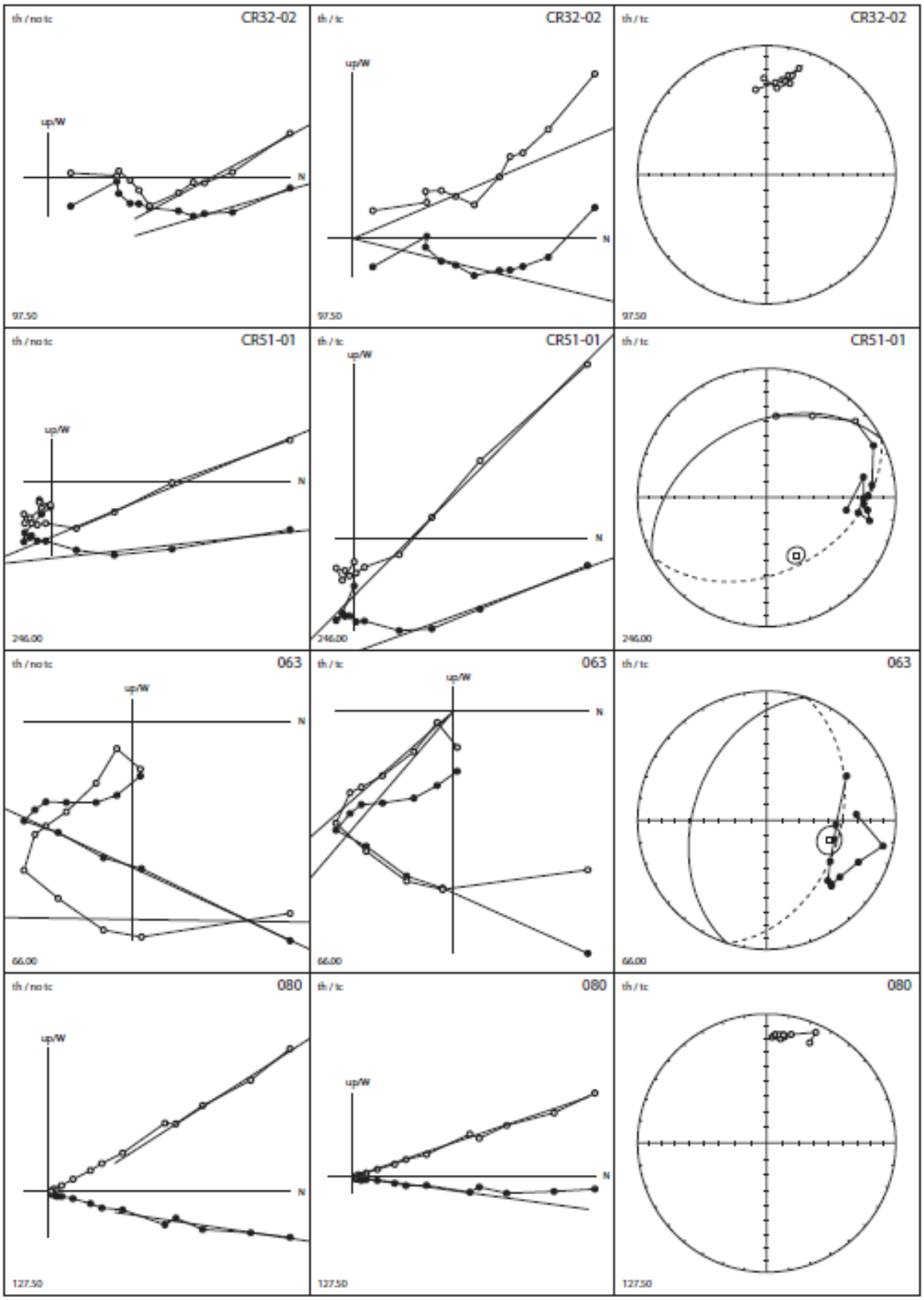
th / no tc
CR32-02
up/W
N
97.50
th / tc
CR32-02
up/W
N
97.50
th / tc
CR32-02
97.50
th / no tc
CR51-01
up/W
N
246.00
th / tc
CR51-01
up/W
N
246.00
th / tc
CR51-01
246.00
th / no tc
063
up/W
N
66.00
th / tc
063
up/W
N
66.00
th / tc
063
66.00
th / no tc
080
up/W
N
127.50
th / tc
080
up/W
N
127.50
th / tc
080
127.50

Figure 9

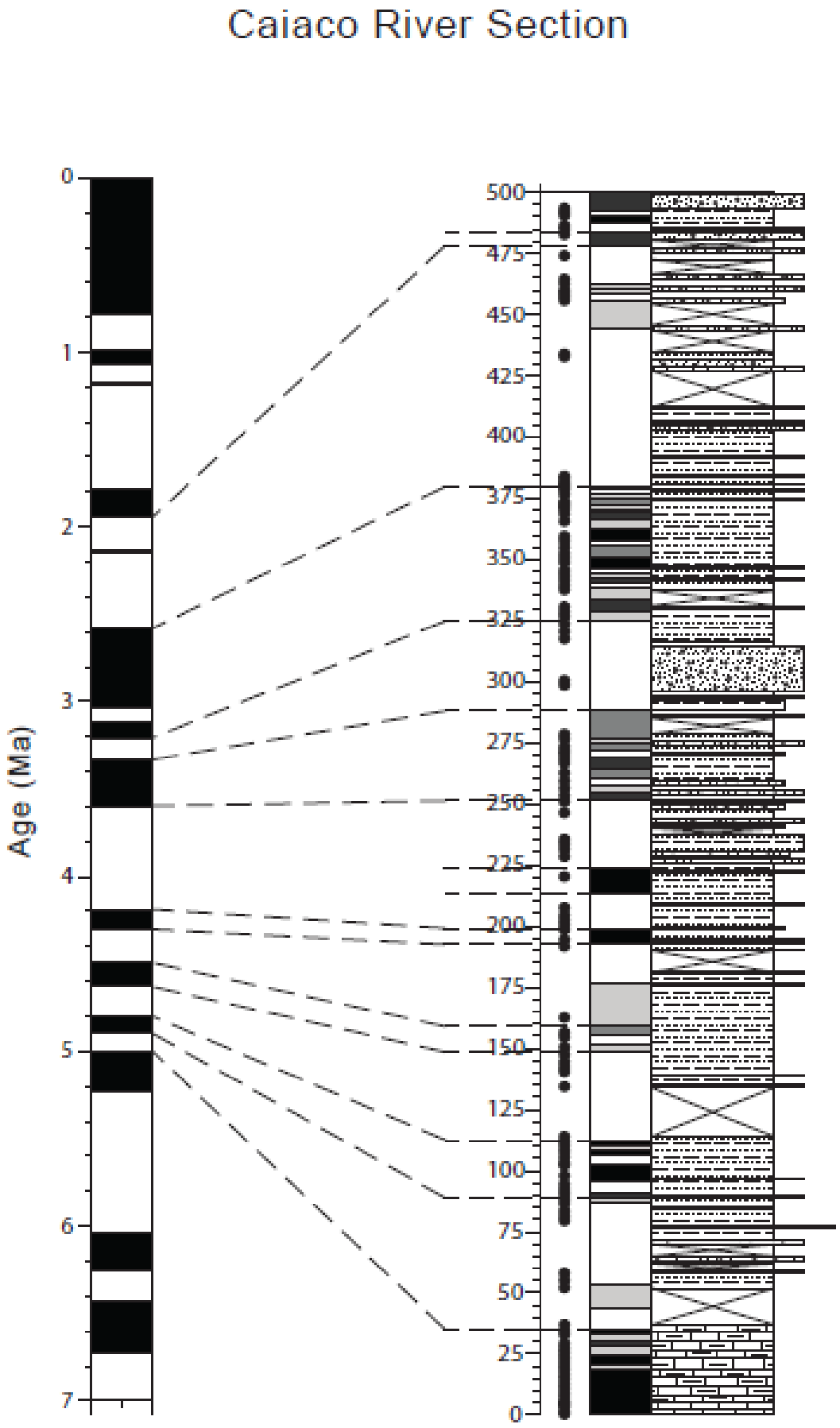
Caiaco River Section
Age (Ma)
0
1
2
3
4
5
6
7
500
475
450
425
400
375
350
325
300
275
250
225
200
175
150
125
100
75
50
25
0

Figure 10.

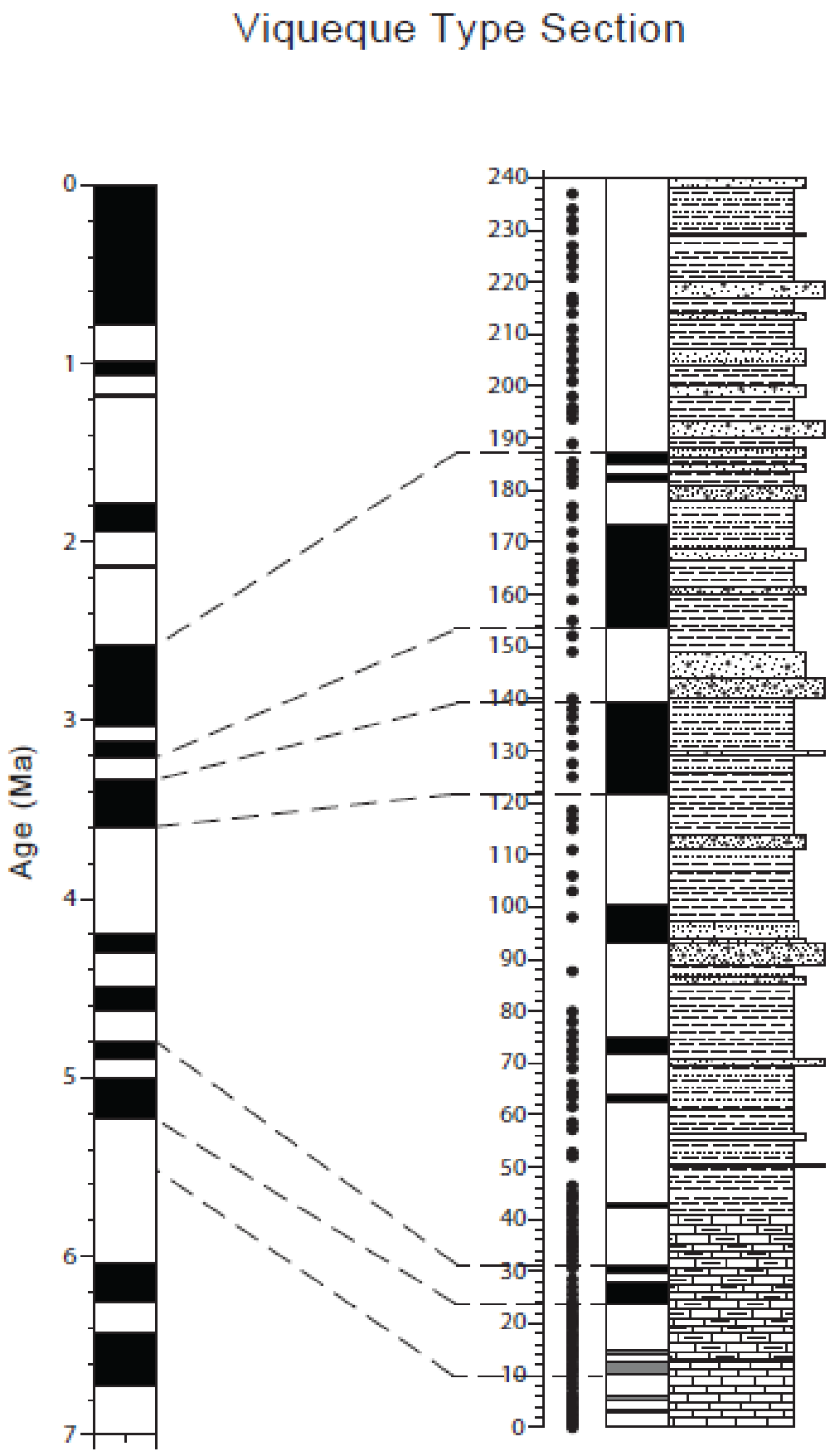
Viqueque Type Section
Age (Ma)
0
1
2
3
4
5
6
7
240
230
220
210
200
190
180
170
160
150
140
130
120
110
100
90
80
70
60
50
40
30
20
10
0

Figure 11.

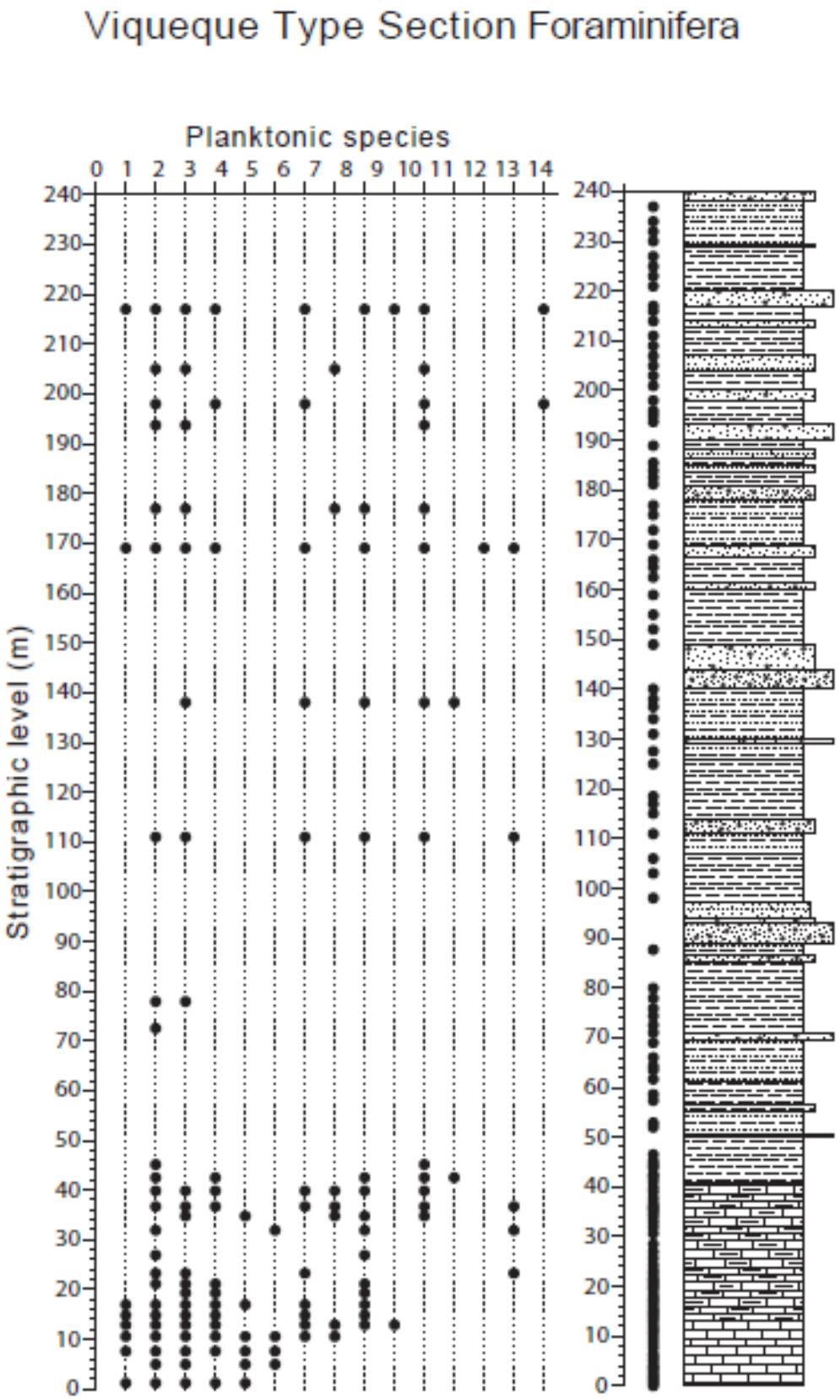
Viqueque Type Section Foraminifera
Planktonic species
0 1 2 3 4 5 6 7 8 9 10 11 12 13 14
Stratigraphic level (m)
240 230 220 210 200 190 180 170 160 150 140 130 120 110 100 90 80 70 60 50 40 30 20 10 0

Figure 12.

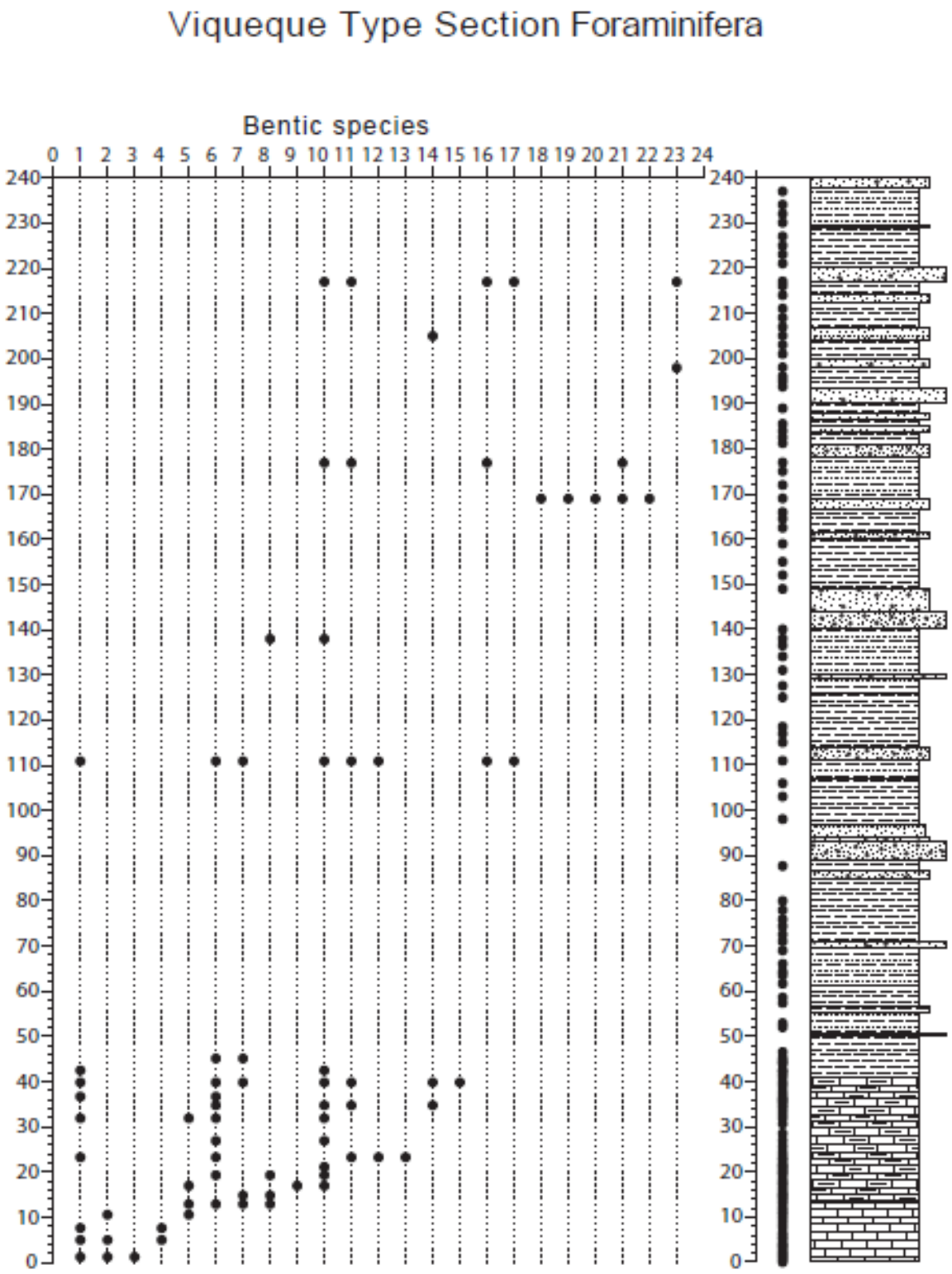
Viqueque Type Section Foraminifera
Bentic species
0 1 2 3 4 5 6 7 8 9 10 11 12 13 14 15 16 17 18 19 20 21 22 23 24
240 230 220 210 200 190 180 170 160 150 140 130 120 110 100 90 80 70 60 50 40 30 20 10 0

Figure 13.

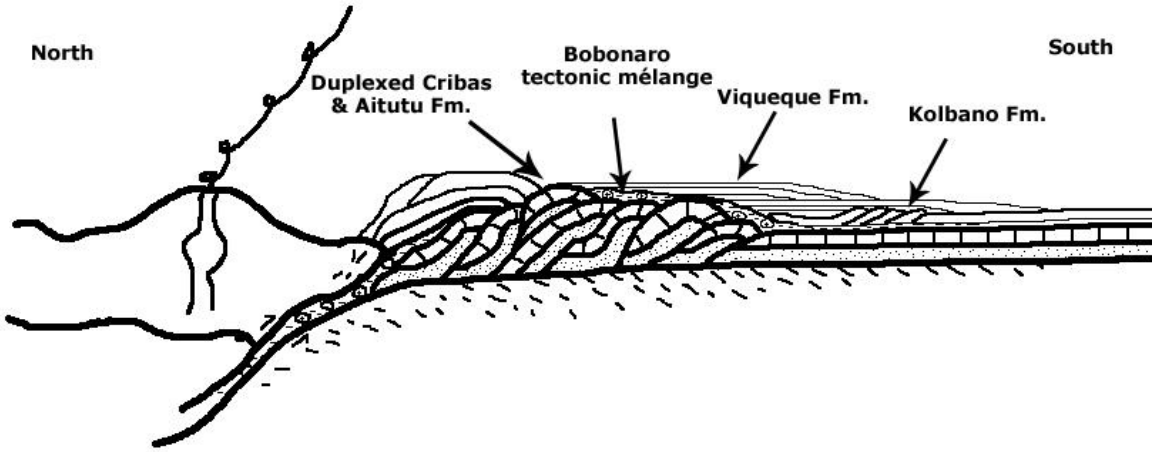
North
Duplexed Cribas
& Aitutu Fm.
Bobonaro
tectonic mélange
Viqueque Fm.
Kolbano Fm.
South

Figure 14.

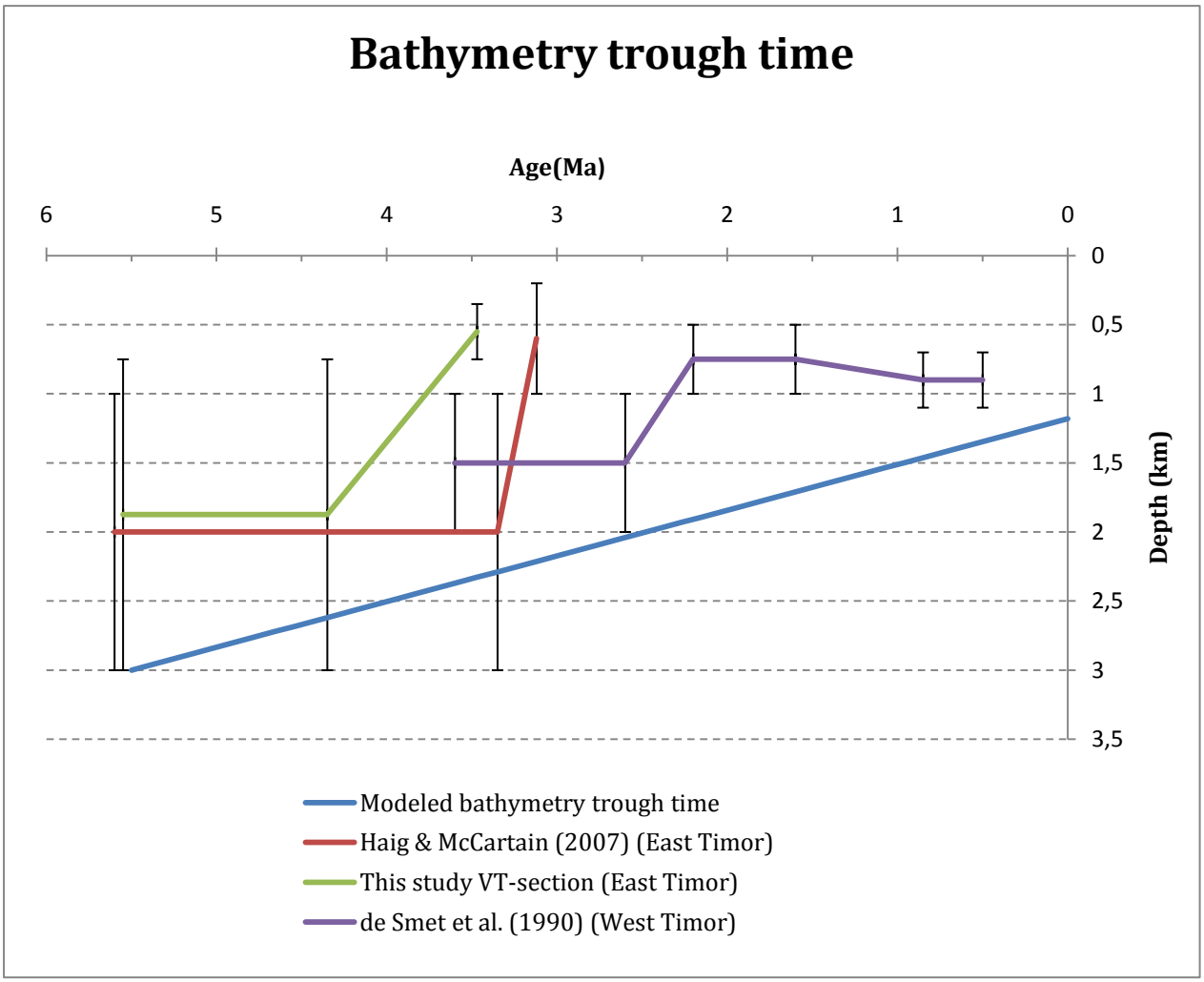
Bathymetry trough time
Age(Ma)
6
5
4
3
2
1
0
0
0,5
1
1,5
2
2,5
3
3,5
Depth (km)
Modeled bathymetry trough time
Haig & McCartain (2007) (East Timor)
This study VT-section (East Timor)
de Smet et al. (1990) (West Timor)

Tables

Table 1.

Variable	Symbol	Value
Density of sediments	ρ_s	2.4 x 10^3 kg m^{-3}
Density of crust	ρ_c	2.8 x 10^3 kg m^{-3}
Density of mantle	ρ_m	3.3 x 10^3 kg m^{-3}
Density of ocean water	ρ_o	1.024 x 10^3 kg m^{-3}
Thickness of sediments	t_s	2.0 km
Thickness of crust	c	20.0 km
Initial water depth	d	3.0 km
Thickness of compensating mantle	m	km
Resulting water depth	h	km
Thickening factor	β	(β >1) -

Appendix

Derivation of equation 1.

Isostatic equilibrium at the moho of the deformed section means that the pressure there is equal. Thus:

$$d\rho_o + t_s\rho_s + c\rho_c + m\rho_m = h\rho_o + \beta t_s\rho_s + c\rho_c \quad \text{(A1)}$$

The variable m can be written as a combination of other thicknesses:

$$m = (h + \beta t_s + c) - (d + t_s + c) \quad \text{(A2)}$$

$$m = h - d + t_s(\beta - 1) \quad \text{(A3)}$$

Substituting (A3) into Equation (A1):

$$d\rho_o + t_s\rho_s + c\rho_c + (h - d + t_s(\beta - 1))\rho_m = h\rho_o + \beta t_s\rho_s + c\rho_c \quad \text{(A4)}$$

rearranging:

$$d\rho_o + t_s\rho_s + (h - d + t_s(\beta - 1))\rho_m = h\rho_o + \beta t_s\rho_s \quad \text{(A5)}$$

$$(d - h)\rho_o + t_s(1 - \beta)\rho_s + (h - d + t_s(\beta - 1))\rho_m = 0 \quad \text{(A6)}$$

$$(d - h)\rho_o + \big(h - d + t_s(\beta - 1)\big)\rho_m = -t_s(1 - \beta)\rho_s \quad \text{(A7)}$$

$$d(\rho_o - \rho_m) + h(\rho_m - \rho_o) + t_s(\beta - 1)\rho_m = t_s(\beta - 1)\rho_s \quad \text{(A8)}$$

$$d(\rho_o - \rho_m) + h(\rho_m - \rho_o) = t_s(\beta - 1)(\rho_s - \rho_m) \quad \text{(A9)}$$

$$h(\rho_m - \rho_o) = t_s(\beta - 1)(\rho_s - \rho_m) - d(\rho_o - \rho_m) \quad \text{(A10)}$$

$$h = \frac{t_s(\beta - 1)(\rho_s - \rho_m) - d(\rho_o - \rho_m)}{\rho_m - \rho_o} \quad \text{(A11)}$$

$$h = \frac{t_s(\beta-1)(\rho_s-\rho_m)}{\rho_m-\rho_o} + d \quad \text{(A12)}$$

Additional note: as shown with the crust, the lithosphere does not play a role in the derivation of equation 1 (see the cancellation at step A4 to A5). Therefore this part has not been taken up into the derivation of his model.